Cell Research (2018) 28:249-252.

www.nature.com/cr

LETTER TO THE EDITOR

Endothelial-specific m^{6}A modulates mouse hematopoietic stem and progenitor cell development via Notch signaling

Cell Research (2018) **28**:249-252. doi:10.1038/cr.2017.143; published online 17 November 2017

Hematopoietic stem and progenitor cells (HSPCs) have been documented to be specified from hemogenic endothelial (HE) cells in the ventral wall of the dorsal aorta (DA) through the endothelial-to-hematopoietic transition (EHT) during mouse embryogenesis [1]. N^6-methyl-adenosine (m^{6}A) is the most prevalent mRNA modification in eukaryotes. Although the function of m^{6}A modification in cell fate determination of embryonic stem cells has been recently reported [2], the physiological role and the underlying mechanism of m^{6}A modification in definitive hematopoiesis during mouse embryogenesis have not been reported yet. Due to the early lethality of mutant mice with conventional knockout of *methyltransferase like 3* (*Mettl3*) [2], one of the most important m^{6}A methyltransferase catalytic subunits identified so far [3], here we utilized *Vec-Cre* mice crossed with *Mettl3$^{fl/fl}$* mice to deplete the expression of Mettl3 specifically in endothelial cells of mouse aorta-gonad-mesonephros (AGM) region.

First, the knockout efficiency of *Mettl3* in endothelial cells of *Vec-Cre*; *Mettl3$^{fl/fl}$* AGM was validated by multiple approaches. The expression of Mettl3 in the whole AGM was significantly decreased at both protein and mRNA levels (Figure 1A; Supplementary information, Figure S1A). The obvious decrease of Mettl3 in endothelial cells of AGM was also confirmed by immunofluorescence (Supplementary information, Figure S1B). Then the developmental hematopoietic phenotype was examined. Interestingly, the expression of *Runx1* and *Gfi1*, both specifically expressed in the intra-aortic hematopoietic cluster and essential for HSPC development [4, 5], was decreased in E10.5 *Vec-Cre*; *Mettl3$^{fl/fl}$* AGM (Figure 1B). This is consistent with the reduced number of Runx1$^+$ cells and hematopoietic clusters by immunofluorescence (Figure 1C). In addition, the proportion of HSPCs (CD34$^+$c-Kit$^+$) in the E10.5 *Vec-Cre*; *Mettl3$^{fl/fl}$* AGM was apparently attenuated as compared to that in the control (Figure 1D). To further testify whether the hematopoietic phenotype was due to endothelial cell-specific depletion of *Mettl3*, *Vav-Cre*; *Mettl3$^{fl/fl}$* embryo, in which the expression of *Mettl3* was specifically deleted in hematopoietic cells, was used as a control. Immunofluorescence results showed that there were no obvious changes in the Runx1$^+$ cell number and hematopoietic cluster formation in the E10.5 *Vav-Cre*; *Mettl3$^{fl/fl}$* AGM (Supplementary information, Figure S1C). Moreover, flow cytometry analysis also indicated that the proportion of HSPCs (CD34$^+$c-Kit$^+$) in the *Vav-Cre*; *Mettl3$^{fl/fl}$* AGM was similar to that in the control (Supplementary information, Figure S1D). Meanwhile, we also examined the percentage of pre-HSCs, the maturation of which is required for the formation of definitive HSCs [6]. Intriguingly, the proportion of pre-HSCs (CD144$^+$CD45$^+$c-Kit$^+$) was dramatically reduced in the E10.5 *Vec-Cre*; *Mettl3$^{fl/fl}$* AGM but was unaltered in the E10.5 *Vav-Cre*; *Mettl3$^{fl/fl}$* AGM as compared with that in controls (Supplementary information, Figure S1E and S1F). Since the earliest HSPCs are derived from HE cells in the AGM region, we then examined the development of HE cells. As expected, the proportion of HE (CD31$^+$c-Kit$^+$) cells was decreased in the E10.5 *Vec-Cre*; *Mettl3$^{fl/fl}$* AGM, but not in the E10.5 *Vav-Cre*; *Mettl3$^{fl/fl}$* AGM and controls (Figure 1E; Supplementary information, Figure S1G). Finally, to determine whether endothelial-specific loss of Mettl3 affects the function of HSPC, we performed the colony-forming unit culture (CFU-C) assay as well as transplantation assay. As shown in Figure 1F and 1G, the colony formation ability and the short-term reconstitution capability of HSPCs in the E10.5 *Vec-Cre*; *Mettl3$^{fl/fl}$* AGM were diminished, suggesting that the function of HSPC was also impaired. Nevertheless, HSPCs functioned normally in the E10.5 *Vav-Cre*; *Mettl3$^{fl/fl}$* AGM (Supplementary information, Figure S1H and S1I). Taken together, these data demonstrate that Mettl3 in endothelial cells of AGM plays a pivotal role in HSPC development during mouse definitive hematopoiesis.

Our recent data showed that Mettl3-mediated m^{6}A modification on *notch1a* mRNA could repress the arterial-endothelial Notch activity to promote HSPC specification in zebrafish [7]. Furthermore, previous studies in zebrafish and mouse showed that the inhibition of Notch signaling in HE cells facilitated EHT and enhanced the generation of HSPCs [8, 9]. To determine whether Notch signaling pathway is regulated by Mettl3 during mouse definitive hematopoiesis, we performed RNA-seq using

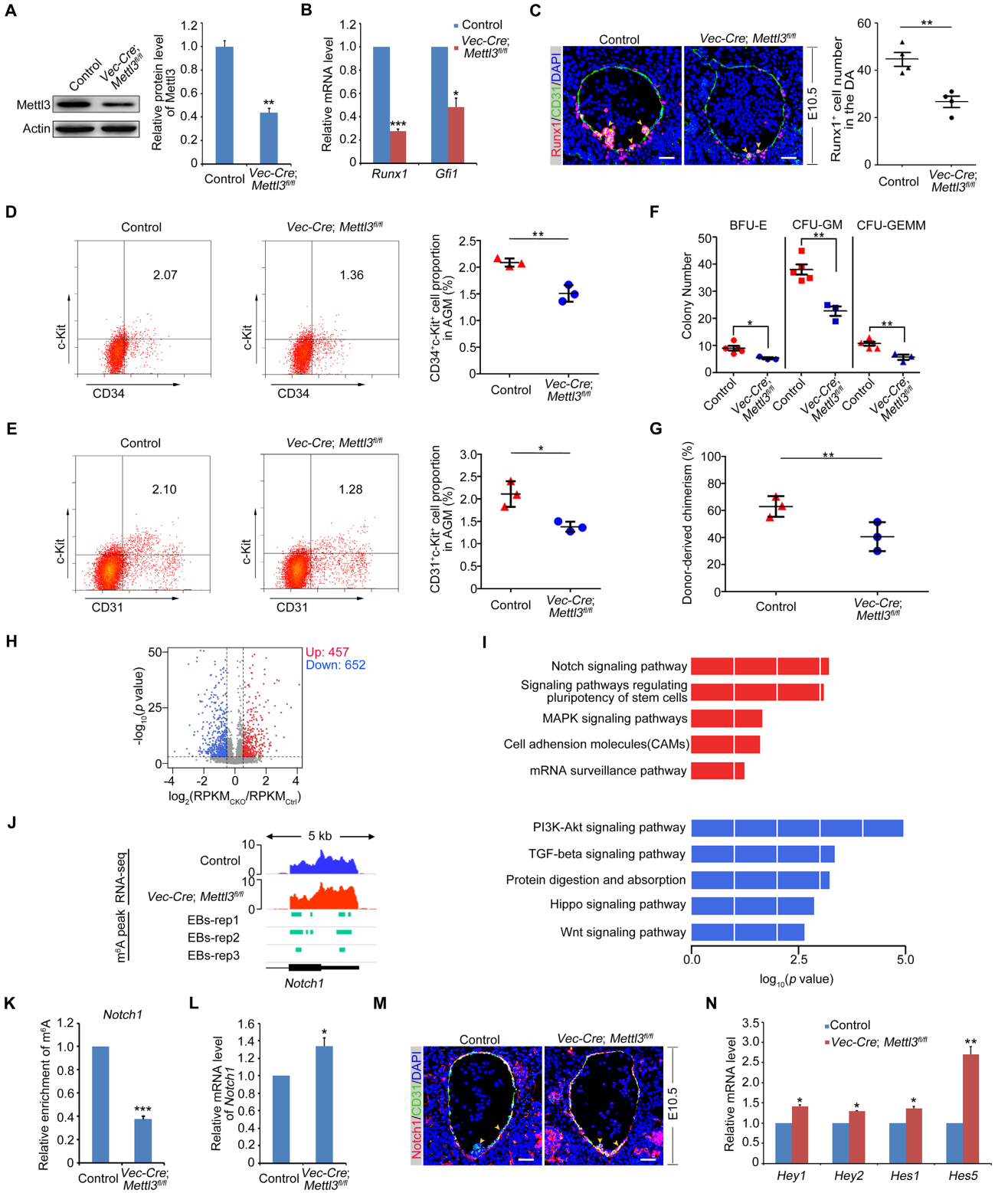
A
Control
Vec-Cre; Mettl3fl/fl
Mettl3
Actin
Relative protein level of Mettl3
Control
Vec-Cre; Mettl3fl/fl
B
Relative mRNA level
Control
Vec-Cre; Mettl3fl/fl
Runx1
Gfi1
C
Control
Vec-Cre; Mettl3fl/fl
Runx1/CD31/DAPI
E10.5
Runx1+ cell number in the DA
D
Control
Vec-Cre; Mettl3fl/fl
2.07
1.36
c-Kit
CD34
CD34+c-Kit+ cell proportion in AGM (%)
F
BFU-E
CFU-GM
CFU-GEMM
Colony Number
G
Donor-derived chimerism (%)
E
2.10
1.28
CD31
CD31+c-Kit+ cell proportion in AGM (%)
H
Up: 457
Down: 652
-log10(p value)
log2(RPKMCKO/RPKMCtrl)
I
Notch signaling pathway
Signaling pathways regulating pluripotency of stem cells
MAPK signaling pathways
Cell adhesion molecules(CAMs)
mRNA surveillance pathway
PI3K-Akt signaling pathway
TGF-beta signaling pathway
Protein digestion and absorption
Hippo signaling pathway
Wnt signaling pathway
log10(p value)
J
5 kb
RNA-seq
m6A peak
Control
Vec-Cre; Mettl3fl/fl
EBs-rep1
EBs-rep2
EBs-rep3
Notch1
K
Notch1
Relative enrichment of m6A
L
Relative mRNA level of Notch1
M
Notch1/CD31/DAPI
N
Relative mRNA level
Hey1
Hey2
Hes1
Hes5

the E10.5 control and *Vec-Cre*; *Mettl3*$^{fl/fl}$ AGM. In total, 457 upregulated and 652 downregulated genes were identified in the *Vec-Cre*; *Mettl3*$^{fl/fl}$ AGM (Figure 1H). As expected, among the upregulated ones, genes that encode components of Notch signaling pathway were highly enriched (Figure 1I). The gene-set enrichment analysis (GSEA) also revealed a marked upregulation of genes in Notch signaling pathway (Supplementary information, Figure S2A). Furthermore, the majority of mRNA transcripts of these genes involved in Notch signaling pathway contained m^{6}A modifications (Supplementary information, Figure S2B), suggesting that m^{6}A might play an important regulatory role in Notch signaling activity. Among these m^{6}A-modified genes, we found that *Hes5*, *Dtx4*, *Dll3*, *Dll1*, *Mfng* and *Nocth1* were remarkably upregulated upon *Mettl3* deficiency (Supplementary information, Figure S2C). Similar to the m^{6}A methylation of *notch1a* mRNA in zebrafish [7], we also identified conserved m^{6}A peak near the stop codon of *Notch1* mRNA (Figure 1J). In addition, m^{6}A-RIP-qPCR assay showed that the enrichment of m^{6}A on *Notch1* mRNA was notably decreased in the E10.5 *Vec-Cre*; *Mettl3*$^{fl/fl}$ AGM (Figure 1K). Subsequently, the increased expression of *Notch1* was observed at mRNA level (Figure 1L). Consistently, immunofluorescence results further showed that in wild-type embryos, Notch1 was only enriched in the endothelial cells but not in the emerging hematopoietic clusters, whereas the increased expression of Notch1 was observed in both endothelial cells and poorly formed hematopoietic clusters in the E10.5 *Vec-Cre*; *Mettl3*$^{fl/fl}$ AGM (Figure 1M). A list of Notch signaling downstream targets including *Hey1*, *Hey2*, *Hes1* and *Hes5* were significantly increased in the E10.5 *Vec-Cre*; *Mettl3*$^{fl/fl}$ AGM detected by qPCR (Figure 1N). In addition, both the mRNA and protein levels of Dll4 were increased in the AGM of *Vec-Cre*; *Mettl3*$^{fl/fl}$ embryo (Supplementary information, Figure S2D-S2F). *Dll4* is not only a downstream target gene of Notch signaling, but also a well-established arterial marker. The increased expression of Dll4 and Notch1 in the AGM of *Vec-Cre*; *Mettl3*$^{fl/fl}$ embryo indicated that Notch signaling was over-activated and the enhanced arterial-endothelial identity inhibited the transition from HE cells to HSPCs. Taken together, endothelial-specific Mettl3 facilitates m^{6}A methylation on *Notch1* mRNA to inhibit Notch activity in HE cells, thereby promoting HSPC generation through EHT.

In summary, we utilized Cre/LoxP system to generate the endothelial-specific knockout mice of *Mettl3*, and identified the indispensable function of Mettl3-mediated m^{6}A modification in mouse definitive hematopoiesis. Mechanistically, endothelial expression of Mettl3 can methylate *Notch1* mRNA and then lead to the repression of Notch activity during EHT. Interestingly, bioinformatics analysis showed that m^{6}A peak near the stop codon of *Notch1* mRNA can be recognized by Ythdf2 (Supplementary information, Figure S2G), suggesting that Ythdf2-mediated *Notch1* mRNA decay is responsible for the observed HSPC phenotype [10]. These results are consistent with our recent findings in zebrafish [7], supporting an evolutionally conserved function of m^{6}A in HSPC specification in mammals. In addition, three recent studies have demonstrated that mRNA m^{6}A modification mediated by Mettl3/Mettl14 plays essential roles during spermatogenesis in mice [11-13], further confirming a

Figure 1 Endothelial-specific deletion of Mettl3 impairs definitive hematopoiesis via Notch signaling during mouse embryogenesis. **(A)** Expression of Mettl3 in the E10.5 control and *Vec-Cre*; *Mettl3*$^{fl/fl}$ AGM detected by western blotting. The right panel is the quantification of the western blotting results. **(B)** qPCR analysis of mRNA levels of *Runx1* and *Gfi1* in the E10.5 control and *Vec-Cre*; *Mettl3*$^{fl/fl}$ AGM. **(C)** Immunofluorescence on the sections of the control and *Vec-Cre*; *Mettl3*$^{fl/fl}$ AGM at E10.5 with anti-Runx1 and anti-CD31 antibodies. Yellow arrowheads mark hematopoietic clusters. The right panel is the quantification of Runx1 positive cells in the DA. **(D**, **E)** Flow cytometry analysis of the percentages of HSPCs (CD34$^+$c-Kit$^+$) and HE (CD31$^+$c-Kit$^+$) cells in the E10.5 AGM of *Vec-Cre*; *Mettl3*$^{fl/fl}$ embryos compared with control. **(F)** CFU-C assays to detect the colony-forming ability of HSPC in the control and *Vec-Cre*; *Mettl3*$^{fl/fl}$ embryos. **(G)** Donor-derived chimerism in peripheral blood (PB) of recipients 4 weeks post transplantation (n = 3 for each group). **(H)** Volcano plot showing differentially expressed genes upon *Mettl3* deficiency. Genes with significantly increased and decreased expression levels were highlighted using red and blue. **(I)** Representative Kyoto Encyclopedia of Genes and Genomes (KEGG) of upregulated (top) or downregulated (bottom) genes in the signaling pathway upon *Mettl3* deficiency. **(J)** Integrative Genomics Viewer (IGV) tracks displaying RNA-seq reads distribution in the E10.5 control (blue) and *Vec-Cre*; *Mettl3*$^{fl/fl}$ (red) AGM and m^{6}A peaks (green) (m^{6}A peak data were downloaded from GSE61995 [2]) at the *Notch1* last exon. **(K)** m^{6}A-RIP-qPCR assay to show the enrichment of m^{6}A on *Notch1* mRNA in the AGM of *Vec-Cre*; *Mettl3*$^{fl/fl}$ embryo at E10.5 compared with control. **(L)** The mRNA level of *Notch1* in the E10.5 control and *Vec-Cre*; *Mettl3*$^{fl/fl}$ AGM by qPCR. **(M)** Expression of Notch1 in the E10.5 control and *Vec-Cre*; *Mettl3*$^{fl/fl}$ AGM by immunofluorescence assay. **(N)** Expression of Notch signaling target genes *Hey1*, *Hey2*, *Hes1* and *Hes5* in the E10.5 control and *Vec-Cre*; *Mettl3*$^{fl/fl}$ AGM. Student's *t*-test: *P < 0.05; **P < 0.01; ***P < 0.001. Scale bar, 10 μm. The statistical results are presented as mean ± SEM. BFU-E, burst-forming unit-erythroid; CFU-GEMM, CFU-granulocyte, erythroid, macrophage, megakaryocyte; CFU-GM, CFU-granulocyte, macrophage. CKO, conditional knockout (*Vec-Cre*; *Mettl3*$^{fl/fl}$); Ctrl, control.

general regulatory role of Mettl3-mediated m^{6}A modification in multiple tissues.

Acknowledgments

This work was supported by grants from the National Natural Science Foundation of China (31425016 and 81530004), the Ministry of Science and Technology of China (2016YFA0100500) and the Strategic Priority Research Program of the Chinese Academy of Sciences, China (XDA01010110).

Junhua Lv[1, 4, *], Yifan Zhang[1, 4, *], Suwei Gao[1, 5, *], Chunxia Zhang[1, 4, *], Yusheng Chen[3, 4, *], Wei Li[2, 4], Yun-Gui Yang[3, 4], Qi Zhou[2, 4], Feng Liu[1, 4]

[1]State Key Laboratory of Membrane Biology, Institute of Zoology, Chinese Academy of Sciences, Beijing 100101, China; [2]State Key Laboratory of Stem Cell and Reproduction Biology, Institute of Zoology, Chinese Academy of Sciences, Beijing 100101, China; [3]CAS Key Laboratory of Genomic and Precision Medicine, Collaborative Innovation Center of Genetics and Development, College of Future Technology, Beijing Institute of Genomics, Chinese Academy of Sciences, Beijing 100101, China; [4]University of Chinese Academy of Sciences, Beijing 100049, China; [5]College of Life Sciences, Hebei University, Baoding 071002, China
*These five authors contributed equally to this work.
Correspondence: Feng Liu
Tel: +86 1064807307; Fax: +86 1064807313
E-mail: liuf@ioz.ac.cn

References

1 Boisset JC, van Cappellen W, Andrieu-Soler C, *et al*. *Nature* 2010; **464**:116-120.
2 Geula S, Moshitch-Moshkovitz S, Dominissini D, *et al. Science* 2015; **347**:1002-1006.
3 Ping XL, Sun BF, Wang L, *et al. Cell Res* 2014; **24**:177-189.
4 Chen MJ, Yokomizo T, Zeigler BM, *et al*. *Nature* 2009; **457**:887-891.
5 Thambyrajah R, Mazan M, Patel R, *et al. Nat Cell Biol* 2016; **18**:21-32.
6 Taoudi S, Gonneau C, Moore K, *et al. Cell Stem Cell* 2008; **3**:99-108.
7 Zhang C, Chen Y, Sun B, *et al. Nature* 2017; **549**:273-276.
8 Zhang P, He Q, Chen D, *et al. Cell Res* 2015; **25**:1093-1107.
9 Lizama CO, Hawkins JS, Schmitt CE, *et al*. *Nat Commun* 2015; **6**:7739.
10 Wang X, Lu Z, Gomez A, *et al. Nature* 2014; **505**:117-120.
11 Hsu PJ, Zhu Y, Ma H, *et al. Cell Res* 2017; **27**:1115-1127.
12 Lin Z, Hsu PJ, Xing X, *et al. Cell Res* 2017; **27**:1216-1230.
13 Xu K, Yang Y, Feng GH, *et al. Cell Res* 2017; **27**:1100-1114.

(**Supplementary information** is linked to the online version of the paper on the *Cell Research* website.)